

Proceedings of the 12th International Conference on
Computational Fluid Dynamics in the Oil & Gas,
Metallurgical and Process Industries

Progress in Applied CFD – CFD2017



SINTEF Proceedings

Editors:

Jan Erik Olsen and Stein Tore Johansen

Progress in Applied CFD – CFD2017

Proceedings of the 12th International Conference on Computational Fluid Dynamics
in the Oil & Gas, Metallurgical and Process Industries

SINTEF Academic Press

SINTEF Proceedings no 2

Editors: Jan Erik Olsen and Stein Tore Johansen

Progress in Applied CFD – CFD2017

Selected papers from 10th International Conference on Computational Fluid Dynamics in the Oil & Gas, Metallurgical and Process Industries

Key words:

CFD, Flow, Modelling

Cover, illustration: Arun Kamath

ISSN 2387-4295 (online)

ISBN 978-82-536-1544-8 (pdf)

© Copyright SINTEF Academic Press 2017

The material in this publication is covered by the provisions of the Norwegian Copyright Act. Without any special agreement with SINTEF Academic Press, any copying and making available of the material is only allowed to the extent that this is permitted by law or allowed through an agreement with Kopinor, the Reproduction Rights Organisation for Norway. Any use contrary to legislation or an agreement may lead to a liability for damages and confiscation, and may be punished by fines or imprisonment

SINTEF Academic Press

Address: Forskningsveien 3 B
 PO Box 124 Blindern
 N-0314 OSLO

Tel: +47 73 59 30 00

Fax: +47 22 96 55 08

www.sintef.no/byggforsk

www.sintefbok.no

SINTEF Proceedings

SINTEF Proceedings is a serial publication for peer-reviewed conference proceedings on a variety of scientific topics.

The processes of peer-reviewing of papers published in SINTEF Proceedings are administered by the conference organizers and proceedings editors. Detailed procedures will vary according to custom and practice in each scientific community.

PREFACE

This book contains all manuscripts approved by the reviewers and the organizing committee of the 12th International Conference on Computational Fluid Dynamics in the Oil & Gas, Metallurgical and Process Industries. The conference was hosted by SINTEF in Trondheim in May/June 2017 and is also known as CFD2017 for short. The conference series was initiated by CSIRO and Phil Schwarz in 1997. So far the conference has been alternating between CSIRO in Melbourne and SINTEF in Trondheim. The conferences focuses on the application of CFD in the oil and gas industries, metal production, mineral processing, power generation, chemicals and other process industries. In addition pragmatic modelling concepts and bio-mechanical applications have become an important part of the conference. The papers in this book demonstrate the current progress in applied CFD.

The conference papers undergo a review process involving two experts. Only papers accepted by the reviewers are included in the proceedings. 108 contributions were presented at the conference together with six keynote presentations. A majority of these contributions are presented by their manuscript in this collection (a few were granted to present without an accompanying manuscript).

The organizing committee would like to thank everyone who has helped with review of manuscripts, all those who helped to promote the conference and all authors who have submitted scientific contributions. We are also grateful for the support from the conference sponsors: ANSYS, SFI Metal Production and NanoSim.

Stein Tore Johansen & Jan Erik Olsen



Organizing committee:

Conference chairman: Prof. Stein Tore Johansen

Conference coordinator: Dr. Jan Erik Olsen

Dr. Bernhard Müller

Dr. Sigrid Karstad Dahl

Dr. Shahriar Amini

Dr. Ernst Meese

Dr. Josip Zoric

Dr. Jannike Solsvik

Dr. Peter Witt

Scientific committee:

Stein Tore Johansen, SINTEF/NTNU

Bernhard Müller, NTNU

Phil Schwarz, CSIRO

Akio Tomiyama, Kobe University

Hans Kuipers, Eindhoven University of Technology

Jinghai Li, Chinese Academy of Science

Markus Braun, Ansys

Simon Lo, CD-adapco

Patrick Segers, Universiteit Gent

Jiyuan Tu, RMIT

Jos Derksen, University of Aberdeen

Dmitry Eskin, Schlumberger-Doll Research

Pär Jönsson, KTH

Stefan Pirker, Johannes Kepler University

Josip Zoric, SINTEF

CONTENTS

PRAGMATIC MODELLING	9
On pragmatism in industrial modeling. Part III: Application to operational drilling	11
CFD modeling of dynamic emulsion stability	23
Modelling of interaction between turbines and terrain wakes using pragmatic approach	29
FLUIDIZED BED	37
Simulation of chemical looping combustion process in a double looping fluidized bed reactor with cu-based oxygen carriers.....	39
Extremely fast simulations of heat transfer in fluidized beds.....	47
Mass transfer phenomena in fluidized beds with horizontally immersed membranes	53
A Two-Fluid model study of hydrogen production via water gas shift in fluidized bed membrane reactors	63
Effect of lift force on dense gas-fluidized beds of non-spherical particles	71
Experimental and numerical investigation of a bubbling dense gas-solid fluidized bed	81
Direct numerical simulation of the effective drag in gas-liquid-solid systems	89
A Lagrangian-Eulerian hybrid model for the simulation of direct reduction of iron ore in fluidized beds.....	97
High temperature fluidization - influence of inter-particle forces on fluidization behavior	107
Verification of filtered two fluid models for reactive gas-solid flows	115
BIOMECHANICS.....	123
A computational framework involving CFD and data mining tools for analyzing disease in carotid artery	125
Investigating the numerical parameter space for a stenosed patient-specific internal carotid artery model.....	133
Velocity profiles in a 2D model of the left ventricular outflow tract, pathological case study using PIV and CFD modeling.....	139
Oscillatory flow and mass transport in a coronary artery.....	147
Patient specific numerical simulation of flow in the human upper airways for assessing the effect of nasal surgery.....	153
CFD simulations of turbulent flow in the human upper airways	163
OIL & GAS APPLICATIONS	169
Estimation of flow rates and parameters in two-phase stratified and slug flow by an ensemble Kalman filter	171
Direct numerical simulation of proppant transport in a narrow channel for hydraulic fracturing application	179
Multiphase direct numerical simulations (DNS) of oil-water flows through homogeneous porous rocks	185
CFD erosion modelling of blind tees	191
Shape factors inclusion in a one-dimensional, transient two-fluid model for stratified and slug flow simulations in pipes	201
Gas-liquid two-phase flow behavior in terrain-inclined pipelines for wet natural gas transportation	207

NUMERICS, METHODS & CODE DEVELOPMENT	213
Innovative computing for industrially-relevant multiphase flows	215
Development of GPU parallel multiphase flow solver for turbulent slurry flows in cyclone.....	223
Immersed boundary method for the compressible Navier–Stokes equations using high order summation-by-parts difference operators	233
Direct numerical simulation of coupled heat and mass transfer in fluid-solid systems	243
A simulation concept for generic simulation of multi-material flow, using staggered Cartesian grids.....	253
A cartesian cut-cell method, based on formal volume averaging of mass, momentum equations.....	265
SOFT: a framework for semantic interoperability of scientific software	273
 POPULATION BALANCE	 279
Combined multifluid-population balance method for polydisperse multiphase flows	281
A multifluid-PBE model for a slurry bubble column with bubble size dependent velocity, weight fractions and temperature.....	285
CFD simulation of the droplet size distribution of liquid-liquid emulsions in stirred tank reactors	295
Towards a CFD model for boiling flows: validation of QMOM predictions with TOPFLOW experiments	301
Numerical simulations of turbulent liquid-liquid dispersions with quadrature-based moment methods.....	309
Simulation of dispersion of immiscible fluids in a turbulent couette flow	317
Simulation of gas-liquid flows in separators - a Lagrangian approach.....	325
CFD modelling to predict mass transfer in pulsed sieve plate extraction columns	335
 BREAKUP & COALESCENCE	 343
Experimental and numerical study on single droplet breakage in turbulent flow	345
Improved collision modelling for liquid metal droplets in a copper slag cleaning process	355
Modelling of bubble dynamics in slag during its hot stage engineering.....	365
Controlled coalescence with local front reconstruction method	373
 BUBBLY FLOWS	 381
Modelling of fluid dynamics, mass transfer and chemical reaction in bubbly flows	383
Stochastic DSMC model for large scale dense bubbly flows.....	391
On the surfacing mechanism of bubble plumes from subsea gas release.....	399
Bubble generated turbulence in two fluid simulation of bubbly flow	405
 HEAT TRANSFER	 413
CFD-simulation of boiling in a heated pipe including flow pattern transitions using a multi-field concept	415
The pear-shaped fate of an ice melting front	423
Flow dynamics studies for flexible operation of continuous casters (flow flex cc).....	431
An Euler-Euler model for gas-liquid flows in a coil wound heat exchanger.....	441
 NON-NEWTONIAN FLOWS.....	 449
Viscoelastic flow simulations in disordered porous media	451
Tire rubber extrudate swell simulation and verification with experiments	459
Front-tracking simulations of bubbles rising in non-Newtonian fluids.....	469
A 2D sediment bed morphodynamics model for turbulent, non-Newtonian, particle-loaded flows.....	479

METALLURGICAL APPLICATIONS.....	491
Experimental modelling of metallurgical processes	493
State of the art: macroscopic modelling approaches for the description of multiphysics phenomena within the electroslag remelting process	499
LES-VOF simulation of turbulent interfacial flow in the continuous casting mold	507
CFD-DEM modelling of blast furnace tapping	515
Multiphase flow modelling of furnace tapholes	521
Numerical predictions of the shape and size of the raceway zone in a blast furnace.....	531
Modelling and measurements in the aluminium industry - Where are the obstacles?	541
Modelling of chemical reactions in metallurgical processes.....	549
Using CFD analysis to optimise top submerged lance furnace geometries	555
Numerical analysis of the temperature distribution in a martensic stainless steel strip during hardening.....	565
Validation of a rapid slag viscosity measurement by CFD.....	575
Solidification modeling with user defined function in ANSYS Fluent.....	583
Cleaning of polycyclic aromatic hydrocarbons (PAH) obtained from ferroalloys plant.....	587
Granular flow described by fictitious fluids: a suitable methodology for process simulations	593
A multiscale numerical approach of the dripping slag in the coke bed zone of a pilot scale Si-Mn furnace.....	599
INDUSTRIAL APPLICATIONS	605
Use of CFD as a design tool for a phosphoric acid plant cooling pond	607
Numerical evaluation of co-firing solid recovered fuel with petroleum coke in a cement rotary kiln: Influence of fuel moisture	613
Experimental and CFD investigation of fractal distributor on a novel plate and frame ion-exchanger	621
COMBUSTION	631
CFD modeling of a commercial-size circle-draft biomass gasifier.....	633
Numerical study of coal particle gasification up to Reynolds numbers of 1000.....	641
Modelling combustion of pulverized coal and alternative carbon materials in the blast furnace raceway	647
Combustion chamber scaling for energy recovery from furnace process gas: waste to value	657
PACKED BED.....	665
Comparison of particle-resolved direct numerical simulation and 1D modelling of catalytic reactions in a packed bed	667
Numerical investigation of particle types influence on packed bed adsorber behaviour	675
CFD based study of dense medium drum separation processes	683
A multi-domain 1D particle-reactor model for packed bed reactor applications.....	689
SPECIES TRANSPORT & INTERFACES	699
Modelling and numerical simulation of surface active species transport - reaction in welding processes	701
Multiscale approach to fully resolved boundary layers using adaptive grids.....	709
Implementation, demonstration and validation of a user-defined wall function for direct precipitation fouling in Ansys Fluent.....	717

FREE SURFACE FLOW & WAVES	727
Unresolved CFD-DEM in environmental engineering: submarine slope stability and other applications.....	729
Influence of the upstream cylinder and wave breaking point on the breaking wave forces on the downstream cylinder	735
Recent developments for the computation of the necessary submergence of pump intakes with free surfaces	743
Parallel multiphase flow software for solving the Navier-Stokes equations	752
 PARTICLE METHODS	 759
A numerical approach to model aggregate restructuring in shear flow using DEM in Lattice-Boltzmann simulations	761
Adaptive coarse-graining for large-scale DEM simulations.....	773
Novel efficient hybrid-DEM collision integration scheme.....	779
Implementing the kinetic theory of granular flows into the Lagrangian dense discrete phase model.....	785
Importance of the different fluid forces on particle dispersion in fluid phase resonance mixers	791
Large scale modelling of bubble formation and growth in a supersaturated liquid.....	798
 FUNDAMENTAL FLUID DYNAMICS	 807
Flow past a yawed cylinder of finite length using a fictitious domain method	809
A numerical evaluation of the effect of the electro-magnetic force on bubble flow in aluminium smelting process.....	819
A DNS study of droplet spreading and penetration on a porous medium.....	825
From linear to nonlinear: Transient growth in confined magnetohydrodynamic flows.....	831

COMPARISON OF PARTICLE-RESOLVED DIRECT NUMERICAL SIMULATION AND 1D MODELLING OF CATALYTIC REACTIONS IN A PACKED BED

Arpit Singhal ^{a, b*}, Schalk Cloete ^c, Stefan Radl ^d, Rosa Quinta-Ferreira ^b and Shahriar Amini ^{a, c}

^a NTNU (Norwegian University of Science and Technology), Department of Energy and Process Engineering, Kolbjørn hejes v 1B, NO-7491, Trondheim, Norway

^b University of Coimbra, Department of Chemical Engineering, Rua Sílvio Lima, Polo II, 3030-790 Coimbra, Portugal

^c SINTEF Materials and Chemistry, Flow Technology Department, S. P. Andersens veg 15 B, NO-7031, Trondheim, Norway

^d TU Graz, Institute of Process and Particle Engineering, 8010 Graz, Inffeldgasse 13/III, Austria

Corresponding author's e-mail: arpit.singhal@ntnu.no

ABSTRACT

The work presents a comparison of catalytic gas-solid reactions in a packed bed as simulated on two widely different scales: direct numerical simulation (capable of accurately predicting transfer phenomena in and around a few particles) and 1D modelling (capable of engineering simulations of industrial scale reactors).

Particle-resolved direct numerical simulation (PR-DNS) is performed on a small geometry containing ~100 realistically packed monodisperse spherical particles generated via the discrete element method (DEM). These results are compared to a 1D packed bed reactor model using the effectiveness factor approach to account for intra-particle mass transfer and a suitable closure for gas-particle heat transfer.

The differences between the results from the two modelling approaches are quantified over a range of Thiele moduli, Prandtl numbers and reaction enthalpies. Results showed that existing 1D-model closures perform well for a simple first order catalytic reaction. Heat transfer completely dominates the overall reaction system when large reaction enthalpies are simulated, while mass transfer limitations dominate at low reaction enthalpies. Future work will extend this comparative approach to packings with more complex particle shapes and complex reactions.

Keywords: Direct numerical simulation (DNS), CFD-DEM, packed bed, catalytic gas-solid reaction, reaction rate, heat transfer, multiscale.

NOMENCLATURE

Greek Symbols

α	Volume fraction
ε	Void fraction
ϕ	Thiele modulus (Th)
η	Effectiveness factor

Latin Symbols

C_p	Specific heat capacity of fluid [J/kg.K]
C_A	Concentration of species A [mol/m ³]
D	Molecular diffusivity [m ² /s]
d_p	Diameter of the cylindrical particle [m]
E	Activation energy [J/mol]
h	Heat transfer coefficient [W/m ² K]
k_0	Arrhenius constant [1/s]

K_f	Thermal Conductivity of fluid [W/m.K]
Nu	Nusselt number (hd_p/K_f)
Pr	Prandtl number ($\mu C_p/K_f$)
R	Gas constant [8.314 J/mol.K]
R_{cat}	Catalytic reaction rate [mol/m ³ s]
r	Radius [m]
Re	Reynolds number ($\rho u_s d_p/\mu$)
T	Temperature [K]
u_s	Superficial velocity of the fluid [m/s].

Sub/superscripts

f	Fluid
s	Solid.
p	Particle.

INTRODUCTION

Gas-solid reaction systems in packed beds are of great industrial influence, with the application widespread from process to metallurgical industries. The catalytic or non-catalytic role of the solid defines the complexity involved in the gas-solid reactions.

There are several advanced models available in literature for gas-solid reaction systems. The non-catalytic reaction systems are considered more complicated as they are transient in nature. The detailed review of such systems is described by (Ramachandran and Doraiswamy, 1982) and more recently by (Nashtae and Khoshandam, 2014). Meanwhile, (Ishida and Wen, 1968) have described the effectiveness factor (η) in catalytic reactions for gas-solid systems. The effectiveness factor in heterogeneous catalyst reaction to obtain the intra particle diffusion in porous particles is suggested in (Levenspiel, 1999).

The recent work from (Yang et al., 2016) described an effectiveness factor for general reaction forms. They presented an analytical expression, which is applicable to wide range of reaction rate forms and provides a direct and computationally efficient approach of obtaining effectiveness factor in packed bed reactors. The validity of such a simplified model when added with heat transfer limitations motivates the current work. Hence, the objective of the work is to obtain a comparison in prediction of effectiveness factor for a catalytic gas-solid reaction on two distinct scales. Firstly, a PR-DNS study of a packed bed of ~100 spherical particles now involving a catalytic reaction based on our previously published work (Singhal et al., 2017) gives insight into a phenomenon of intra particle diffusion along with heat transfer limitations. Secondly, a 1D packed bed reactor model coupled with the effectiveness

factor model from (Yang et al., 2016) describes the intra-particle heat and mass transfer. The results obtained from both the approaches are compared and documented.

METHODOLOGY

Thiele Modulus and Effectiveness Factor

The effectiveness factor concept in heterogenous catalytic gas-solid reactions can be explained as the effect of intra particle diffusion on the reaction rate (Ishida and Wen, 1968; Levenspiel, 1999).

$$\eta = \frac{\text{actual reaction rate}}{\text{reaction rate without diffusion limitations}}$$

Thus, the effectiveness factor in catalytic reactions is directly linked with the Thiele modulus (Thiele, 1939). Thiele modulus is explained as:

$$\phi \approx \frac{\text{reaction rate}}{\text{diffusion rate}}$$

PR-DNS Simulation Setup

The spherical particle bed is generated using DEM (Discrete Element Method) integrated in ANSYS FLUENT following the procedure described in the paper (Singhal et al., 2017). The geometry is meshed with fine body-fitted polyhedral elements both inside and outside the particles with resolution of $dp/30$ on the particle surfaces and the growth rate of 20% (Figure 1).

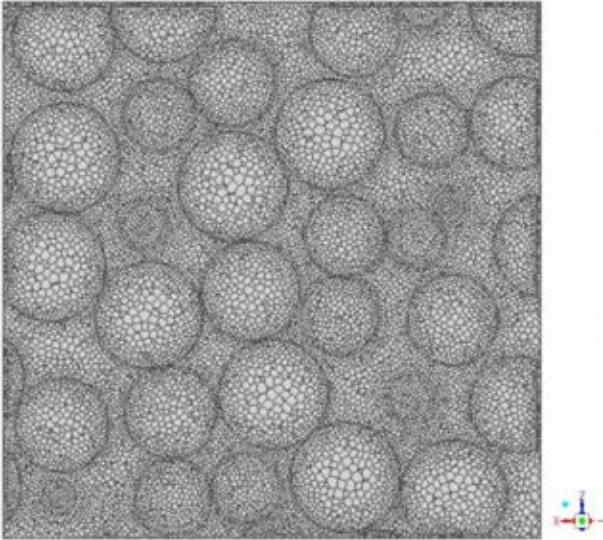
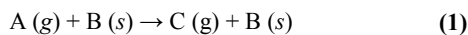


Figure 1: A section ($y = 0$) through the geometry meshed with polyhedral elements.

ANSYS FLUENT is used to complete steady state DNS using the SIMPLE algorithm for pressure-velocity coupling with 2nd order spatial discretization of other equations. Steady state DNS was found to be sufficient for this case since no transient fluctuations occurred in the small spaces between particles (Singhal et al., 2017). The geometry incorporates a velocity inlet, a pressure outlet and a no-slip condition on the wall. The reaction takes place in the porous solid particles (grain model (Szekely, 1976)) modelled by the Eq. (1). The simulation parameters used in the DNS simulations are describe in the Table 1.



The reaction rate is described in the conventional way:

$$R_{cat} = \alpha_s k C_A \quad (2)$$

$$k = k_0 \exp\left(\frac{-E}{RT}\right) \quad (3)$$

Simulations were completed at three different levels of mass transfer resistance (Thiele modulus), heat transfer resistance (Prandtl number) and reaction enthalpy as outlined in Table 1. Mass and heat transfer was adjusted by setting the molecular diffusivity and gas-phase thermal conductivity according to the Th and Pr numbers specified in Table 1. No solids phase thermal conductivity was included in order to accentuate heat transfer resistances in the particle. For the reaction rate, the pre-exponential factor in Eq. (3) was chosen to result in a reaction rate constant of 10000 1/s at a temperature of 1000 K. A large activation energy is selected to accentuate coupling between heat and mass transfer.

Table 1: Simulation parameters for PR-DNS

Parameters	Value
Particle diameter (d_p) (m)	0.001
Packed bed voidage	0.355
Particle void fraction (internal)	0.3
Density (kg/m^3)	Fluid :1 Particles :2500
Fluid velocity (m/s)	1
Inlet mole fraction (A)	0.1
Specific heat capacity (C_p) ($J/kg/k$)	1000
Thiele moduli (Th)	5, 10, 20
Prandtl numbers (Pr)	0.4, 1.6, 6.4
Heat of reaction (kJ/mol)	100, 10, 0

1D Packed Bed Model

A detailed outline of the setup of the 1D model used in this work can be viewed in a recent work by the authors (Cloete et al., 2016). The model is solved in the commercial CFD code, ANSYS FLUENT 16.2, on a domain with 100 cells arranged in only one direction. In order to simulate a packed bed, the Eulerian Two Fluid Model approach is followed and the velocity of the solids phase is fixed to zero in all cells. Conservation equations for mass, momentum, species and energy are then solved in the conventional manner.

In the present study, the most important closures are the effectiveness factor for modelling intra-particle mass transfer limitations (Levenspiel, 1999) and the gas-particle heat transfer coefficient for modelling external heat transfer limitations (Gunn, 1978). The effectiveness factor for the simple first order catalytic reaction considered in this study is written as follows:

$$\eta = \frac{3}{\phi^2} (\phi \coth(\phi) - 1) \quad (4)$$

$$\phi = r_p \sqrt{\frac{k}{D_e}} \quad (5)$$

$$D_e = \frac{D\varepsilon}{\tau} \quad (6)$$

The Thiele modulus (ϕ) represents the ratio of kinetic rate to diffusion rate, so higher values represent greater mass transfer limitation. The effective diffusivity (D_e) is composed of the molecular diffusivity (D), the void fraction of porous particles ($\varepsilon = 0.3$) and the tortuosity ($\tau = 1$).

The classical Gunn correlation for gas-particle heat transfer is written as follows:

$$Nu = (7 - 10\varepsilon + 5\varepsilon^2) \left(1 + 0.7Re^{0.2}Pr^{\frac{1}{3}} \right) + (1.33 - 2.44\varepsilon) + 1.2\varepsilon^2 Re^{0.7} Pr^{\frac{1}{3}} \quad (7)$$

Inlet and outlet boundary conditions as well as the domain length are set to identical values as the PR-DNS simulations. The solids volume fraction in the bed is taken as the product of

the mean solids volume fraction in the PR-DNS domain (0.645) and the solids volume fraction in the particles (0.7).

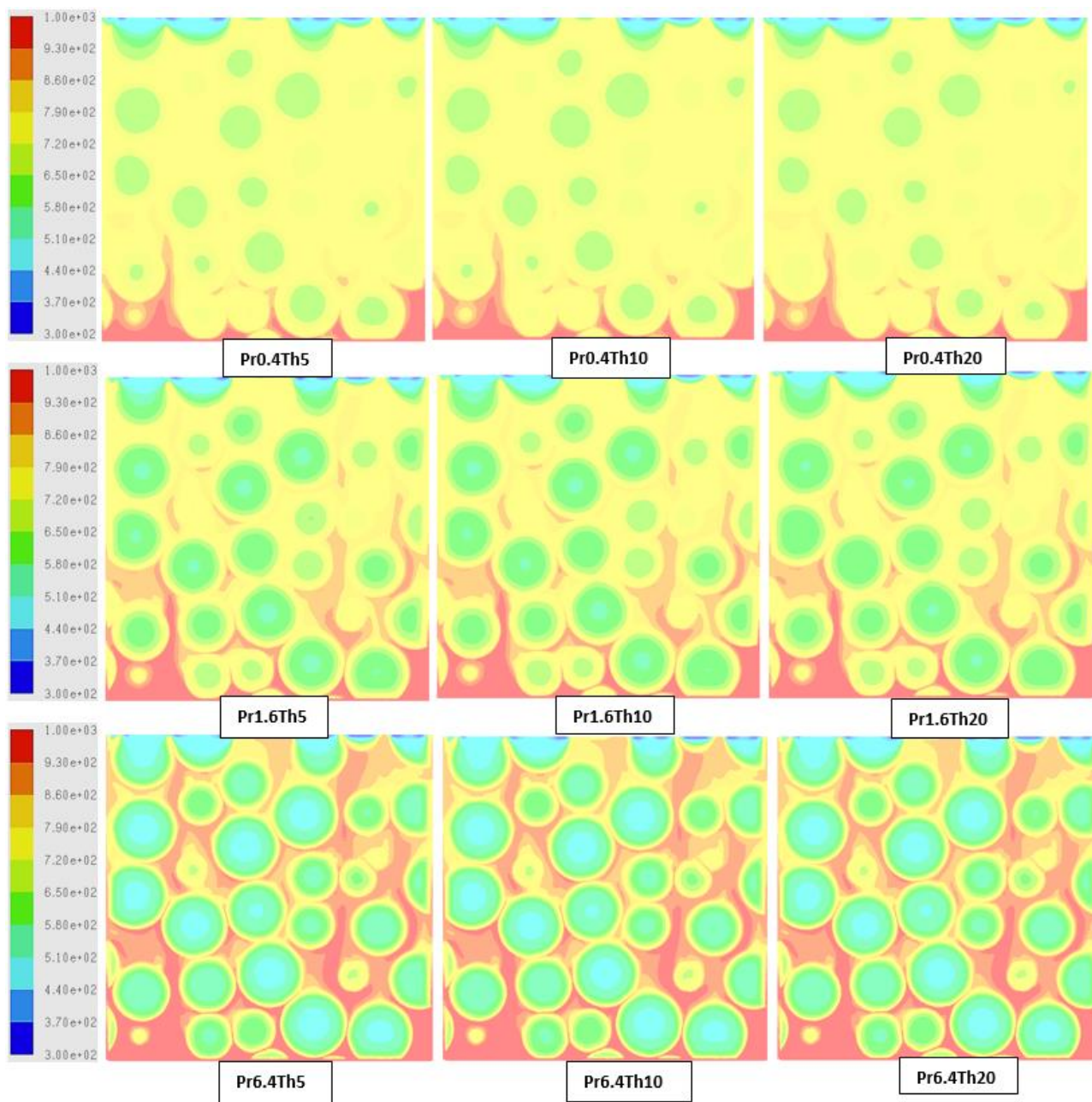


Figure 2: The PR-DNS results for the temperature variation in the packed bed of spherical particles for different Prandtl numbers (Pr) and Thiele moduli (Th)

RESULTS AND DISCUSSIONS

Heat and Mass Transfer in Densely Packed Bed

PR-DNS results for simulations completed with different Thiele moduli and Prandtl numbers for the highly endothermic reaction ($dH_{rxn} = 100$ kJ/mol) are shown in Figure 2 and Figure 3. The temperature variation in Figure 2 illustrates the increasing effect of the heat transfer resistance as Pr is increased by decreasing the gas-phase thermal conductivity. Even though the thermal conductivity is also very low inside the particle, it is clear that external gas-particle heat transfer still dominates.

This is most clearly visible in the Pr6.4 cases in Figure 2 where the temperature gradient inside the particles is small relative to the temperature gradient in the fluid film around the particles. Figure 3 illustrates the mass transfer resistances. It is immediately evident that mass transfer resistances are much less influential in this case than heat transfer resistances because the species concentration gradients are small relative to the temperature gradients in Figure 2. The Pr0.4Th20 case shows some intra-particle mass transfer resistance as a clear species gradient within the particles. The importance of heat transfer resistance relative to mass transfer resistance for this particular case will be further discussed in the next sections.

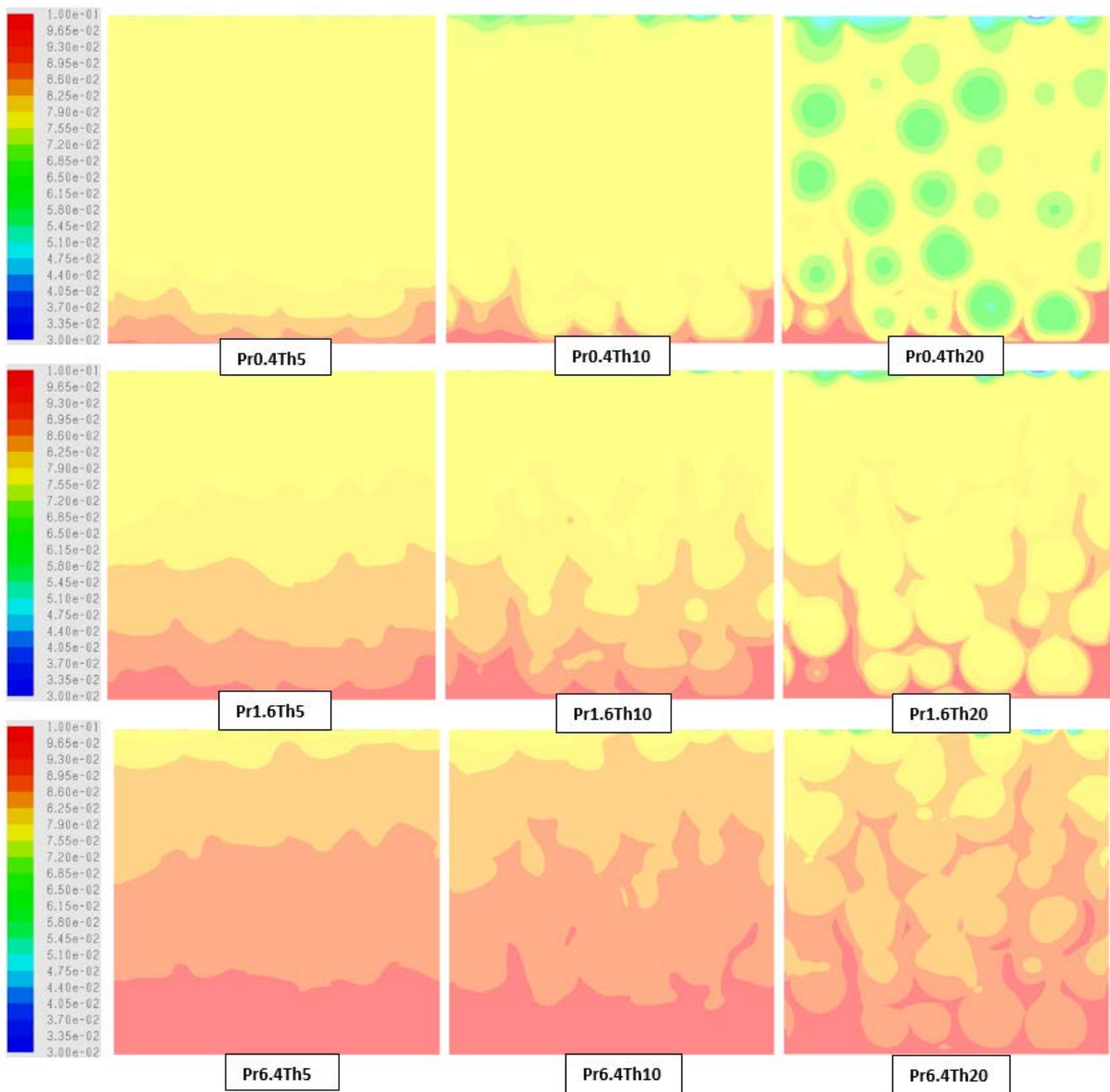


Figure 3: The PR-DNS results for the reactant (A) mole fraction in the packed bed of spherical particles for different Prandtl numbers (Pr) and Thiele moduli (Th).

Individual Particle Data

The PR-DNS approach allows for extraction of detailed data from individual particles within the domain. In this way, the effectiveness factor for individual particles can be extracted and compared. This will be done for the case with the largest heat and mass transfer limitations (Th20-Pr6.4). The definition of the effectiveness factor becomes very important in this case. Three different approaches will be followed (Figure 4):

- **Species:** Comparing the species concentration on the particle surface to the average concentration in the particle (the effectiveness factor for an isothermal first order reaction)
- **Surface:** Comparing the average reaction rate in the particle to the reaction rate that would occur using species concentration and temperature on the particle surface.
- **Volume:** The same as the previous point, only using data averaged over the volume of the particle.

The fact that the “species” effectiveness factor is close to unity implies that mass transfer plays essentially no role in this particular case (the reactant concentration on the particle surface is essentially the same as the reactant concentration in the particle volume). This case is therefore almost exclusively controlled by heat transfer (as seen in the Th20-Pr6.4 case of Figure 2 and Figure 3).

The heat transfer limitation becomes clear when looking at the “surface” effectiveness factor. The temperature on the particle surface is a lot higher than inside the particle volume where the reaction takes place. Calculating the reaction based on the particle surface temperature would therefore result in large errors.

Interestingly, the “volume” effectiveness factor is larger than unity. This implies that there is a significant amount of temperature variation inside the particle, brought about by the assumption of zero thermal conductivity by the solid material. Naturally, this will not be the case in most catalyst particles, but it presents an interesting phenomenon. Given the exponential increase in reaction kinetics with temperature, any variation in temperature around the mean will strongly increase the average

kinetic rate inside the particle. This is what happened in this case: the actual reaction rate inside the particle was higher than the reaction rate calculated based on the average particle temperature.

1D Model Predictions

Comparisons between PR-DNS and 1D model results are discussed in this section. Firstly, the 1D model will be compared to PR-DNS results over a range of Prandtl numbers and Thiele moduli. Secondly, the reaction enthalpy will be changed and the models will be compared again. Finally, an important observation regarding the implementation of the 1D model will be presented.

Variation of Prandtl number and Thiele modulus

A comparison of axial reactant concentration is given in Figure 5 for nine combinations Prandtl number and Thiele modulus. It is clear that the 1D model successfully predicts the PR-DNS results.

In addition, the dominance of heat transfer limitations is clear in all cases because results for different Thiele moduli are essentially identical, whereas results for different Prandtl numbers differ substantially. As may be expected, the amount of reaction in this endothermic system decreases as Pr is increased by decreasing the gas phase thermal conductivity. A lower thermal conductivity implies greater gas-particle heat transfer resistance, thereby allowing less heat to enter and sustain the highly endothermic reaction.

The continued dominance of heat transfer resistance at $Pr = 0.4$ is interesting given the clear intra-particle species gradients that can be observed in the Th20-Pr0.4 case in Figure 2. This is because the outer shell of the particles is slightly hotter than the centre, implying that reduced species concentrations in the centre of the particle (where the temperature is lower and the kinetics is slower) does not have such a large impact on the overall reaction rate.

Figure 6 shows the axial evolution of the difference between the average gas temperature and the average particle temperature. Again, it is clear that mass transfer limitations are essentially negligible, while gas-particle heat transfer dominates the system.

In this case, there is a clear deviation between the PR-DNS and 1D-simulation results: PR-DNS consistently predicts a larger difference between the average gas and particle temperatures. This implies that the PR-DNS predicts a lower particle temperature than the 1D simulations (gas temperature reduces with gas species concentration and is almost identical between the PR-DNS and 1D simulations). As mentioned in the previous section, the temperature variation inside the particle in the PR-DNS allows the reaction rate to be higher than that implied by the average particle temperature. On the other hand, the 1D simulation inherently assumes constant temperature in all particles. For this reason, the two models predict the same overall reaction rate at different average particle temperatures.

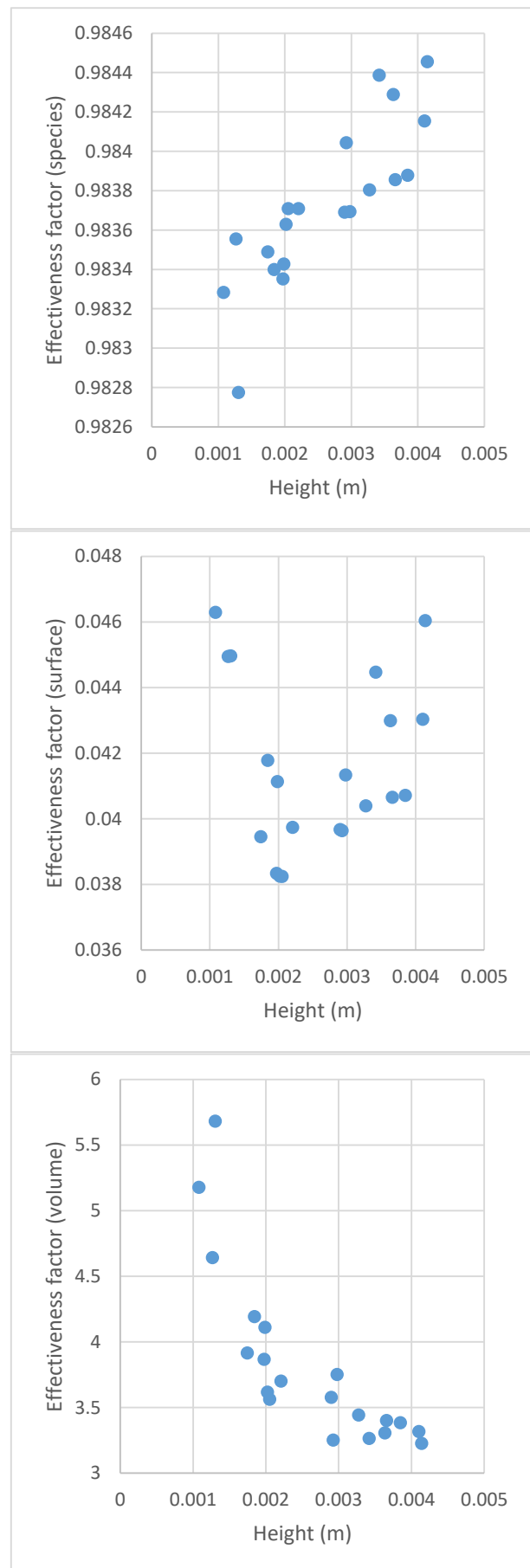


Figure 4: Three different representations of effectiveness factors for 20 particles from the Th20-P6.4 case.

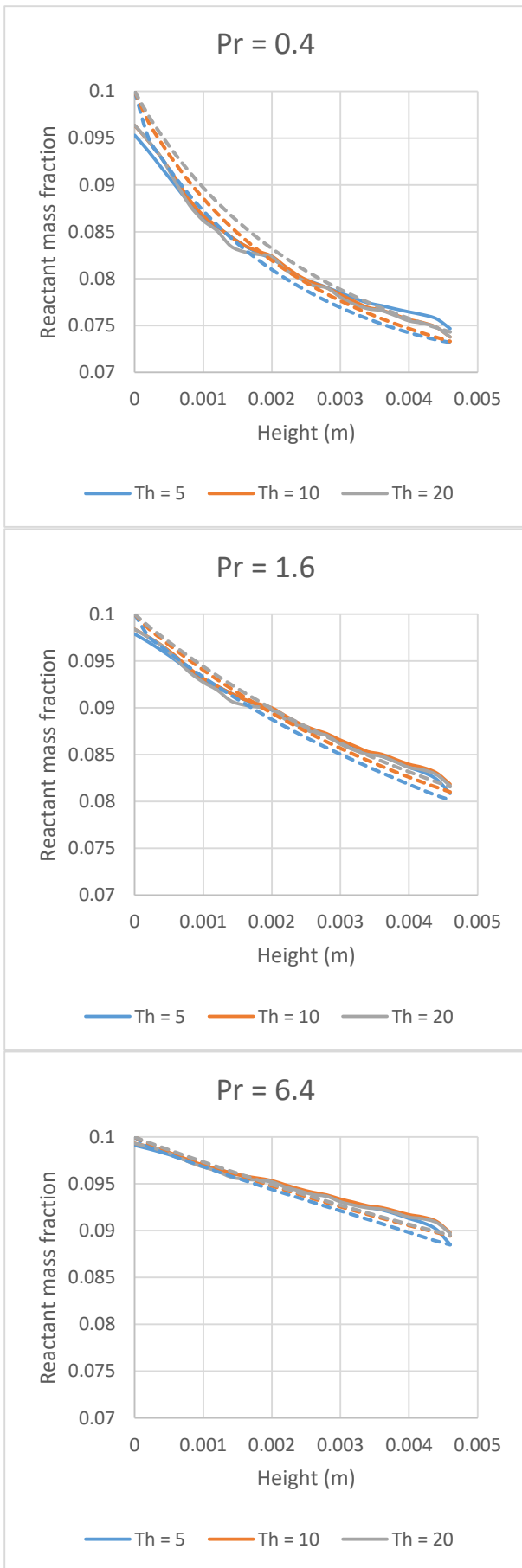


Figure 5: Comparison of axial species profiles between PR-DNS (solid lines) and 1D simulations (dashed lines) for different Prandtl numbers (Pr) and Thiele moduli (Th).

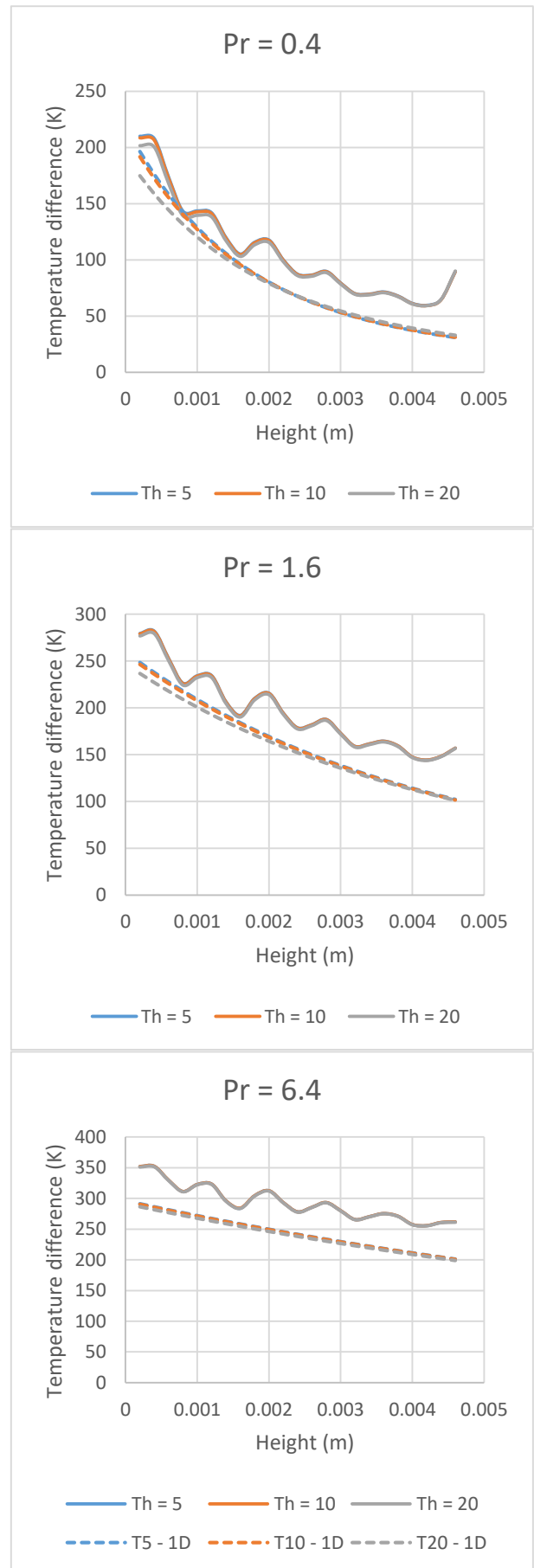


Figure 6: Comparison of axial gas-particle temperature difference between PR-DNS (solid lines) and 1D simulations (dashed lines) for different Prandtl numbers (Pr) and Thiele moduli (Th).

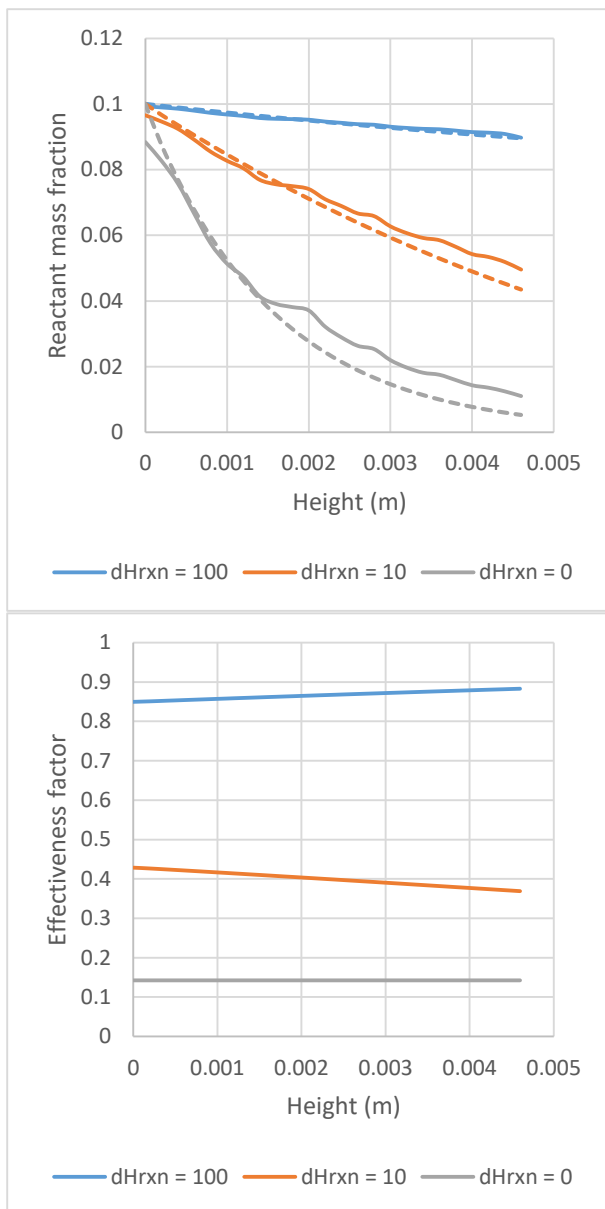


Figure 7: Comparison of axial species profiles between PR-DNS (solid lines) and 1D simulations (dashed lines) for different reaction enthalpies (dH_{rxn} in kJ/mol). The effectiveness factor predicted by the 1D model is also shown for the different cases.

Variation of reaction enthalpy

Results in the previous section were generated with a strongly endothermic reaction ($dH_{rxn} = 100$ kJ/mol). This section will investigate three additional reaction enthalpies on the case with the greatest mass and heat transfer resistances (Th20-Pr6.4). Figure 7 shows the effect of reaction enthalpy on the reactant conversion. It is clear that a decrease in the reaction enthalpy greatly increased reactant conversion and that the 1D model accurately predicts the results from PR-DNS.

The increase in conversion with a decrease in the endothermicity of the reaction is simply due to the large heat transfer resistances included in this case. As the reaction becomes less endothermic, the requirement for heat flow into the particle reduces, thereby lessening the impact of this limitation. As a result, mass transfer becomes the controlling phenomenon, as can be seen from the reduction in the effectiveness factor in Figure 7.

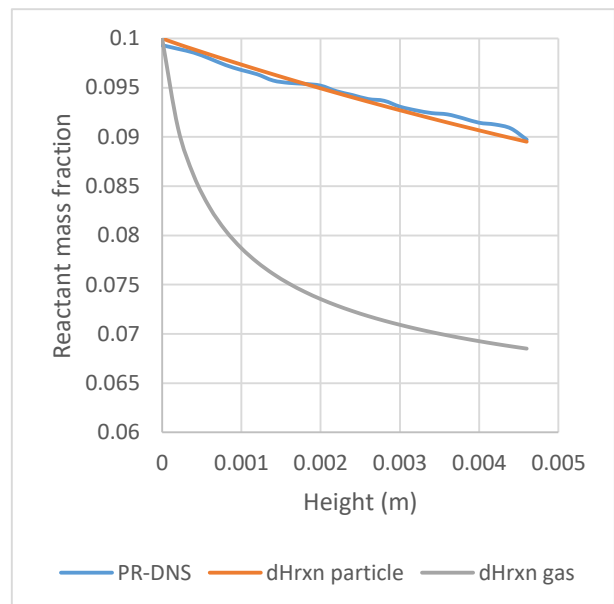


Figure 8: Comparison of the 1D simulations to the PR-DNS results illustrating the importance of assigning the reaction heat to the particle phase.

Importance of the reaction enthalpy source term

Finally, an important observation regarding the 1D-modelling of gas-solid reaction systems with significant reaction enthalpies can be shared. It is intuitive to add the energy source term related to a reaction involving gas species to the gas phase, but this results in large errors if significant gas-particle heat transfer limitations exist. To get accurate predictions, all reaction enthalpy must be assigned to the particle phase in the 1D simulation. This practice mimics the real case where all reaction heat is released or consumed within the particle, even if only gas species is involved in the reaction.

As an illustration of the importance of this observation, the axial species profiles from the Th20-Pr6.4 case with $dH_{rxn} = 100$ kJ/mol are presented in Figure 8. It is clear that assigning the reaction heat to the gas phase completely over-predicts the reaction. This is because the large gas-particle heat transfer limitation observed in earlier sections is essentially eliminated if the heat is not extracted in the particle phase.

CONCLUSION

This work presented a comparison of particle-resolved direct numerical simulations (PR-DNS) results with 1D modelling of a reactive gas-particle system with large heat and mass transfer limitations. Existing 1D model closures for intra-particle mass transfer and gas-particle heat transfer compared well to the PR-DNS results. However, it was shown that it is vitally important that all reaction heat must be assigned as a source term in the particle phase, even if only gas species are reacting.

When a highly endothermic reaction ($dH_{rxn} = 100$ kJ/mol) is simulated, gas-particle heat transfer completely dominates the reaction phenomena in the particle assembly. Large heat consumption in the particle requires large quantities of heat to enter the particle from the gas phase. Mass transfer resistances become increasingly important as the reaction enthalpy becomes smaller until the system becomes exclusively mass transfer controlled when no reaction heat is simulated.

It was also interesting to observe that the 1D model still produced good results even though significant intra-particle heat transfer limitations were included to generate some temperature gradients inside the particles. This finding, combined with the knowledge that a constant particle temperature is normally a safe assumption, suggests that good models for external gas-particle heat transfer and internal mass

transfer are sufficient for accurate 1D model predictions of packed bed reactors.

ACKNOWLEDGEMENT

This work is a part of a European Union project under Seventh research framework program (FP7/2007-2013) under grant agreement n° 604656 - A multi-scale Simulation based design platform for Cost effective CO₂ capture Processes using Nano-structured materials (NanoSim). The authors are grateful to European Research Council for its support. Additionally, the computational resources at NTNU provided by NOTUR, <http://www.notur.no>, were used during this project.

REFERENCES

- Cloete, S., Gallucci, F., van Sint Annaland, M., Amini, S., (2016). "Gas Switching as a Practical Alternative for Scaleup of Chemical Looping Combustion". *Energy Technology* **4**, 1286-1298.
- Gunn, D.J., (1978). "Transfer of heat or mass to particles in fixed and fluidised beds". *International Journal of Heat and Mass Transfer* **21**, 467-476.
- Ishida, M., Wen, C.Y., (1968). "Comparison of kinetic and diffusional models for solid-gas reactions". *AIChE Journal* **14**, 311-317.
- Levenspiel, O., (1999). "Chemical Reaction Engineering, 3rd ed". John Wiley & Sons, New York.
- Nashtae, P.S.b., Khoshandam, B., (2014). "Noncatalytic gas-solid reactions in packed bed reactors: a comparison between numerical and approximate solution techniques". *Chemical Engineering Communications* **201**, 120-152.
- Ramachandran, P.A., Doraiswamy, L.K., (1982). "Modeling of noncatalytic gas-solid reactions". *AIChE Journal* **28**, 881-900.
- Singhal, A., Cloete, S., Radl, S., Quinta-Ferreira, R., Amini, S., (2017). "Heat transfer to a gas from densely packed beds of monodisperse spherical particles". *Chemical Engineering Journal* **314**, 27-37.
- Szekely, J., Evans, J.W., Sohn, H.Y., (1976). "Gas-solid reactions". Academic Press, New York.
- Thiele, E.W., (1939). "Relation between Catalytic Activity and Size of Particle". *Industrial & Engineering Chemistry* **31**, 916-920.
- Yang, W., Cloete, S., Morud, J., Amini, S., (2016). "An Effective Reaction Rate Model for Gas-Solid Reactions with High Intra-Particle Diffusion Resistance", *International Journal of Chemical Reactor Engineering*, p. 331.